Possible "new" quantum systems. II. Properties of the isotopes of spin-aligned hydrogen*

M. D. Miller
Department of Physics and Astronomy, University of Massachusetts, Amherst, Massachusetts 01002

L. H. Nosanow†
Division of Materials Research, National Science Foundation, Washington, D.C. 20550
(Received 6 January 1977)

The ground-state and finite-temperature properties of spin-aligned hydrogen and its isotopes (H↑, D↑, T↑) are studied theoretically. Calculations of the ground-state energy are presented for the Kolos-Wolniewicz (KW) potential and compared to those utilizing Lennard-Jones (LJ) and Morse potentials fit to the KW potential. Excellent agreement between the KW and LJ results is found; thus, permitting confirmation of previous predictions that H↑ can *never* form a liquid phase. In addition, spin-aligned deuterium with one ($D\uparrow_1$) and two ($D\uparrow_2$) allowed nuclear spin states is also studied. Ground-state energies and relevant zero-temperature critical parameters are presented for these systems. Additionally, the quantum theorem of corresponding states is used along with the ground-state results to estimate the critical parameters of $D\uparrow_1$ and $D\uparrow_2$. Finally, the effect of quantum mechanics on the critical behavior of these systems is considered and it is concluded that such effects are not likely to be observable.

I. INTRODUCTION AND SUMMARY

In the recent work of Dugan, Etters, and Palmer[1] and Stwalley and Nosanow,[2] it has been shown that a system composed of one of the hydrogen isotopes suitably constrained so that a pair can interact only in the $b\,^3\Sigma_u^+$ state would exhibit even more extreme "quantum" behavior than the helium isotopes. In particular, it is expected that spin-aligned hydrogen H↑ will *never* form a liquid phase. It was, therefore, suggested[1,2] that H↑ would exhibit a Bose-Einstein condensation and would, therefore, be most worthwhile to study experimentally.

The present work is devoted to a further theoretical study of the properties of the various isotopes of spin-aligned hydrogen (H↑, D↑, and T↑). We follow SN and fit the H↑-H↑ interaction with a Lennard-Jones form. Then we can bring to bear techniques and results[3-6] which have been developed to treat related problems within the context of the quantum theorem of corresponding states (QTCS) originally proposed by de Boer[7] and coworkers.[8] The most important parameter of this theorem is the quantum parameter

$$\eta \equiv \hbar/m\epsilon\sigma^2 = (\Lambda^*/2\pi)^2 , \tag{1.1}$$

where Λ^* was introduced by de Boer[7]; the rest of the symbols are defined in Sec. II. One of the main points made in this recent work was that it is most illuminating to think of the quantum parameter η as a "conceptual" thermodynamic variable. In this way, it was possible to show clearly the effect of the "statistics" on the solidification pressure,[3] to understand the liquid-to-gas phase transition in Bose and Fermi systems,[4] to construct[5] the phase diagram for ^{6}He, and to construct[6] the "generalized phase diagram" for quantum systems.

In the present work, these techniques and results are applied to deduce the properties of the various isotopes of spin-aligned hydrogen. In Sec. III, the equations of state of the various isotopes are computed using different potentials and different numerical approximations. In this way the use of a Lennard-Jones potential by SN to approximate the H↑-H↑ interaction is shown to be justified for sufficiently low densities. Thus, their demonstration that H↑ *never* forms a liquid phase is confirmed. Further, in Sec. III, the equation of state of D↑ is studied. Two cases are considered: (i) $D\uparrow_1$, in which only one nuclear-spin state is allowed, and (ii) $D\uparrow_2$, in which two nuclear-spin states are allowed. Our results indicate that both of these systems should be gaseous at zero temperature, but should liquify under pressure. Unfortunately, there are enough approximations in these calculations so that we cannot yet claim to have categorically demonstrated this result. Finally, in Sec. III, we give estimates of the various ground-state critical parameters for Fermi systems that interact via Lennard-Jones potentials with one and two allowed nuclear-spin states. In Sec. IV, we take these last results and experimental data on other quantum systems and use the QTCS to estimate the various critical parameters of $D\uparrow_1$ and $D\uparrow_2$. We also discuss the possibility of observing quantum effects on the critical behavior of these systems. In Sec. II, we discuss the H↑-H↑ interaction and give a brief review of the QTCS to lay the ground work for Secs. III and IV. In the Appendix we give the equations which describe $D\uparrow_1$; those which describe $D\uparrow_2$ may be found, e.g., in MNP.

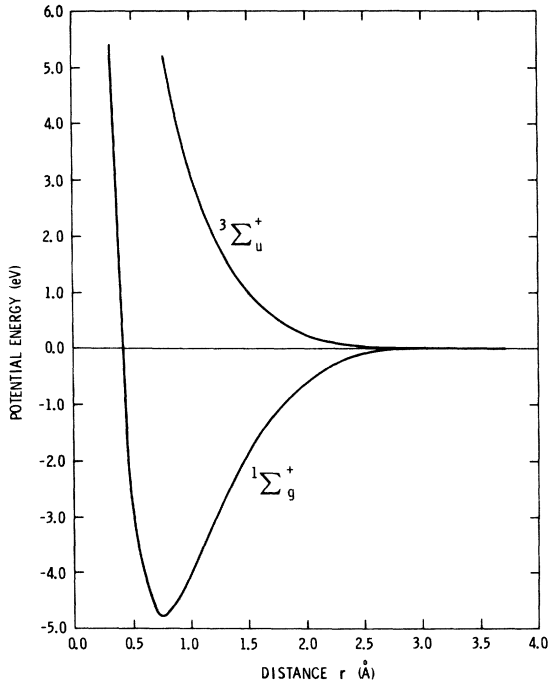

FIG. 1. Potential energy curves for atomic hydrogen in the $X\,^1\Sigma_g^+$ state and the (spin-aligned) $b\,^3\Sigma_g^+$ state as calculated by Kolos and Wolniewicz.

II. PRELIMINARIES

In this section we shall lay the ground work for the following sections. We shall first discuss the H↑-H↑ interaction and then give a brief review of the QTCS.

The H-H pair potentials in the $X\,^1\Sigma_g^+$ and $b\,^3\Sigma_u^+$ states have been very accurately determined by Kolos and Wolniewicz in a pair of extensive variational calculations.[9] We shall refer to these as the Kolos-Wolniewicz (KW) potentials. In Fig. 1 we plot the potential energy curves for two H atoms in these states. The state $X\,^1\Sigma_g^+$ is the usual ground state of the H_2 molecule. The state $b\,^3\Sigma_u^+$ is strongly repulsive at small interatomic separations because of the electronic-spin triplet and has a weak van der Waals attraction. The energy in Fig. 1 is given in units of electron volts so that this weak van der Waals attraction is not discernible.

In Fig. 2 we plot the $b\,^3\Sigma_u^+$ potential with an energy scale of °K. The minimum is clearly discernible with a well depth $\epsilon = 6.46$ °K at a distance $r_m = 4.14$ Å. There is no bound state in this well for atoms as light as the isotopes of hydrogen. This potential energy is the pair interaction between two spin-aligned hydrogen atoms. The KW potential has been shown to be very accurate; thus, spin-aligned hydrogen is an unusual many-body system in that the pair potential is *not* one of the uncertainties in the problem. On Fig. 2 we have also fitted a Lennard-Jones (LJ) potential to the minimum of the KW potential and plotted the He-He interaction for comparison. It is seen that LJ potential provides quite a good fit to the KW potential. Results of calculations with these two potentials are discussed in Sec. III. Since the H↑-H↑ interaction is clearly weaker than the He-He interaction, a glance at Fig. 2 already suggests that H↑ will exhibit more "extreme" quantum behavior than He.

In Table I we display the KW and LJ potentials for a selected number of points. It is clear that, even though the LJ potential is considerably more repulsive at small interatomic spacing, the agreement in the important region around the well is very good. We believe that this is the important characteristic to be required of a potential in order to accurately represent the low-density equation of state. For distances greater than 6.87 Å, we used the following expression for the asymptotic expansion of the polarization energy:

$$v(r) \sim -C_6 r^{-6} - C_8 r^{-8} - C_{10} r^{-10}, \tag{2.1}$$

with the coefficients determined by Bell[10]

$$C_6 = 4.506\times10^4\ ^\circ\mathrm{K}\,\text{Å}^6,$$

$$C_8 = 2.415\times10^5\ ^\circ\mathrm{K}\,\text{Å}^8,$$

$$C_{10} = 1.786\times10^6\ ^\circ\mathrm{K}\,\text{Å}^{10}.$$

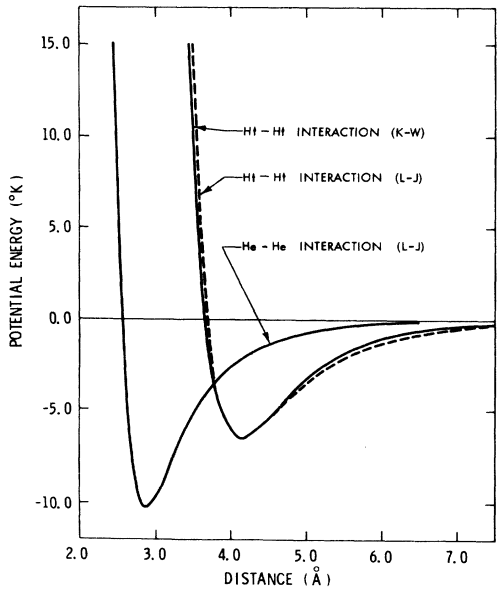

FIG. 2. Kolos-Wolniewicz and Lennard-Jones potentials for H↑ and the Lennard-Jones potential for He. The Lennard-Jones parameters for H↑, $\epsilon = 6.464$ °K and $r_m = 4.141$ Å, were determined to fit the minimum of the Kolos-Wolniewicz potential.

TABLE I. Kolos-Wolniewicz[a] (KW) and the Lennard-Jones (LJ) potentials compared. The LJ parameters are $\epsilon = 6.464$ °K and $r_m = 4.14$ Å. We note that $r_m^*(\mathrm{KW}) = 1.128$ and $r_m^*(\mathrm{LJ}) = 1.122$, where $r_m^* \equiv r_m/\sigma$.

R (Å)	V_{KW} (°K)	V_{LJ} (°K)
0.529	1.195×10^{5}	3.407×10^{11}
0.741	6.816×10^{4}	6.008×10^{9}
0.953	4.159×10^{4}	2.944×10^{8}
1.164	2.531×10^{4}	2.647×10^{7}
1.376	1.512×10^{4}	3.560×10^{6}
1.588	8.839×10^{3}	6.369×10^{5}
1.799	5.055×10^{3}	1.408×10^{5}
2.011	2.824×10^{3}	3.659×10^{4}
2.223	1.538×10^{3}	1.077×10^{4}
2.434	8.131×10^{2}	3.482×10^{3}
2.646	4.153×10^{2}	1.205×10^{3}
2.858	2.022×10^{2}	4.344×10^{2}
3.069	9.177×10	1.571×10^{2}
3.281	3.643×10	5.334×10
3.493	1.027×10	1.396×10
3.704	−1.192	−0.6146
3.916	−5.478	−5.440
4.128	−6.462	−6.462
4.339	−6.063	−6.076
4.551	−5.194	−5.254
4.762	−4.260	−4.378
4.974	−3.418	−3.586
5.186	−2.716	−2.916
5.398	−2.153	−2.367
5.609	−1.712	−1.923
5.821	−1.364	−1.567
6.033	−1.089	−1.281
6.244	−0.8803	−1.053
6.456	−0.7167	−0.8687
6.668	−0.5850	−0.7204
6.879	−0.4809	−0.6002
7.091	−0.3978	−0.5025

[a] The four last KW energies were calculated with the asymptotic expansion formula given by Eq. (2.1).

We shall now give a brief review of the QTCS.[3,6,7] This theorem applies to a class of systems with pair potentials of the form

$$v(r) = \epsilon v^*(r/\sigma)\,, \tag{2.2}$$

where ϵ is the coupling constant (with dimensions of energy), σ is a range parameter (with dimensions of length), and $v^*(x)$ is the same dimensionless function of its argument for each member of this class of systems. For the Lennard-Jones form

$$v^*(r^*) = 4(r^{*-12} - r^{*6})\,. \tag{2.3}$$

To state the QTCS, it is convenient first to introduce the quantum parameter η defined by Eq. (1.1). We have found it notationally more convenient to use η than the de Boer parameter Λ^*. Values of η along with values of ϵ, σ, and other useful quantities are given for various substances in Table II. It is further convenient to introduce several dimensionless or "reduced" variables as follows:

$$T^* \equiv k_B T/\epsilon\,, \tag{2.4a}$$

$$V^* \equiv V/N\sigma^3 = 1/\rho^*\,, \tag{2.4b}$$

$$P^* \equiv P\sigma^3/\epsilon\,, \tag{2.4c}$$

$$F^* \equiv F/N\epsilon\,, \tag{2.4d}$$

where T is the temperature, V is the volume, N is the number of particles, ρ is the number density, P is the pressure, and F is the Helmholtz free energy. The QTCS states that, for a one-component system,

$$F^* = F^*(T^*, V^*, \eta)\,, \tag{2.5}$$

where F^* depends *only* on the form of $v^*(r^*)$ and on whether the particles obey *Bose-Einstein* or *Fermi-Dirac* statistics. A more complete dis-

TABLE II. Quantum parameter η for various substances (H†, D†, and T† denote spin-aligned hydrogen, deuterium, and tritium, respectively). Also given are the masses, coupling constants ϵ, "core diameters" σ, ϵ/σ^3, and $N_0\sigma^3$. We used $\hbar = 1.054\,30\times10^{-27}$ erg sec and $N_0 = 6.022\,52\times10^{23}$ particles/mole.

Substance	m (amu)[a]	ϵ (K)[b]	σ (Å)	ϵ/σ^3 (atm)	$N_0\sigma^3$ (cm^3/mole)	η
H†	1.008	6.46	3.69	17.5	30.2	0.547
D†	2.014	6.46	3.69	17.5	30.2	0.274
^{3}He	3.016	10.22	2.556	83.39	10.06	0.2409
T†	3.016	6.46	3.69	17.5	30.2	0.183
^{4}He	4.003	10.22	2.556	83.39	10.06	0.1815
^{6}He	6.019	10.22	2.556	83.39	10.06	0.1207
H_2	2.016	37.0	2.92	202.5	15.0	0.0763
D_2	4.028	37.0	2.92	202.5	15.0	0.0382
Ne	20.18	35.6	2.74	235.8	12.4	0.0085
Ar	39.95	120.0	3.41	412.3	23.9	0.000 88

[a] 1 amu = $1.660\,24\times10^{-24}$ g.

[b] $k_B = 1.380\,54\times10^{-16}$ erg/particle K.

cussion of the QTCS as it relates to the present work can be found in Refs. 3 and 6.

III. GROUND-STATE RESULTS

In this section we will discuss in detail the zero-temperature properties of the spin-aligned hydrogen isotopes. We shall begin the section by outlining the numerical techniques which were used to calculate the equations of state for systems interacting with KW or LJ potentials. The equations of state will then be presented and compared for both boson and fermion systems. In the Bose case we conclude that, at least at low densities, the LJ potential is a good approximation to the exact KW potential. Thus by using previous results[3-6] on LJ systems we are able to show that H↑ *never* forms a liquid phase; whereas, T↑ is a self-bound liquid at zero pressure. We also present our results for $D\uparrow_1$ and $D\uparrow_2$. They suggest that both of these systems will be *gaseous* in their ground states. However, these results are not conclusive and they will be fully discussed in this section. Finally, a summary of our present estimates of the critical parameters for the ground states of Fermi systems with one or two allowed nuclear-spin states will be given.

Both the boson and fermion systems are treated variationally with trial wave functions ψ of the form

$$\psi = F\Phi\,, \tag{3.1}$$

where

$$F = \prod_{i<j} \exp[\tfrac{1}{2}u(r_{ij})]\,, \tag{3.2}$$

and

$$\Phi = \begin{cases} 1, & \text{for bosons} \\ \mathcal{A}\left(\prod_j e^{i\vec{k}_j\cdot\vec{r}_j}\xi_j\right), & \text{for fermions}\,. \end{cases} \tag{3.3}$$

In Eq. (3.3) $\mathcal{A}$ is the antisymmetrizer and ξ_j is the spin function for particle j. The pair function, $u(r)$, introduces the short-range correlations induced by the strong repulsion at small interatomic distances. It is chosen to have the form

$$u(r) = -(br_m/r)^5\,. \tag{3.4}$$

Therefore, ψ has the proper symmetry for bosons or fermions and upper bounds to the energy can be obtained by evaluating the expectation value of the many-body Hamiltonian.

In the case of a boson system the calculation of the energy is formally analogous to the situation in classical statistical mechanics in the canonical ensemble and those techniques developed for the classical problem can be utilized for the quantum mechanical one. In particular, the problem reduces to obtaining the radial distribution function $g(r)$ generated by ψ. In this paper we shall use $g(r)$'s which are solutions of the Born-Bogoliubov-Green-Kirkwood-Yvon (BBGKY)–Kirkwood-superposition-approximation (KSA) and hypernetted-chain (HNC) approximate integral equations.[11] These equations are approximate in the sense that they sum to all orders a *selected* set of cluster diagrams. For the spin-aligned hydrogen systems, however, we are interested only in the low-density regime where the integral equations are expected to be quite accurate.

The energy expectation value for the fermion system is very complicated due to the presence of the Slater determinant. The effects of statistics can be approximated, however, by use of the cluster expansion introduced by Wu and Feenberg.[12] The application of this technique results in an expression for the fermion energy which is a functional of the associated boson $g(r)$ *only* [that is, that $g(r)$ which is determined by the F part of ψ] and is extensively discussed in MNP. Thus the same set of $g(r)$'s can be used for calculations on both the boson and fermion systems. The explicit expressions for the energy for $D\uparrow_2$ are in MNP and those for $D\uparrow_1$ are in the Appendix.

An additional feature of the fermion D↑ system is the fact that it has a nucleus with spin 1. In this paper we shall concern ourselves with two possible cases: (i) *one* allowed nuclear-spin state ($D\uparrow_1$) and (ii) *two* allowed nuclear-spin states ($D\uparrow_2$) (in this case we assume there are two *equally* populated Fermi seas). In principle, case (i) should be the most important experimentally since the other possibilities allow destruction of H↑ by collisions which can cause electron-spin flip due to the hyperfine interaction and consequent H_2 formation. Case (ii) will be considered, however, because of its theoretical interest and possible experimental interest.

The calculated equations of state are shown in Figs. 3–5. In Fig. 3 we show the results for the boson H↑ and T↑ systems. If we compare the HNC and BBGKY-KSA energies for both systems, we note that the BBGKY results are always lower than the HNC results. However, the energy differences are quite small at low densities. The softness of the BBGKY equation of state relative to the HNC equation of state has previously been noted for the case of helium,[11] where it is also pointed out that the exact molecular dynamics results tend to fall between the two approximations. Thus, we may conclude that the H↑ and T↑ results in Fig. 3 are valid upper bounds to the energies. Next, we note that the agreement between the LJ and KW results is much better for H↑ than for T↑. This is clearly due to the increased importance in the kinetic en-

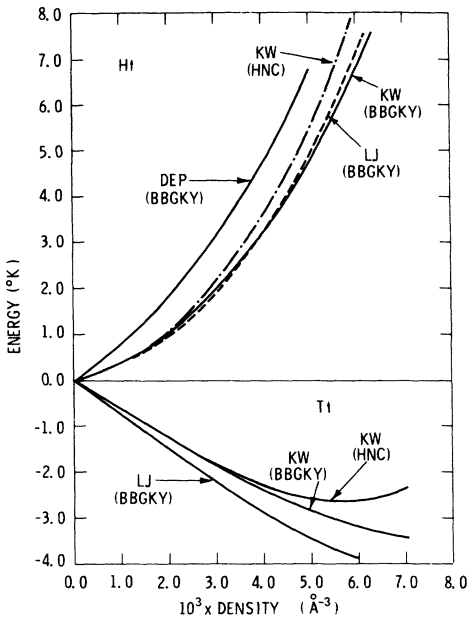

FIG. 3. Energy as a function of density for spin-aligned hydrogen and tritium. The H ↑ results are given for the KW potential with HNC and BBGKY distribution functions and the LJ potential and for the Morse potential used by DEP with the BBGKY distribution functions. As explained in the text, the DEP energies are calculated with a different value of η than the other results. These results clearly show that H ↑ will be a gas at all densities; whereas, T ↑ will be a self-bound liquid.

ergy in the former system which tends to mitigate the difference in the potential energies. In fact since the same $u(r)$ is used for the LJ and KW systems, the *forms* of the kinetic energy will be identical.

The form for Eq. (3.4) was suggested by the LJ potential. The results in Table I clearly show that at small separations the KW potential is not nearly as repulsive as the LJ; thus, it is clear that one could choose a softer pair function which would prevent particles from penetrating the repulsive cores with a smaller kinetic energy price to pay. DEP have investigated this effect for their Morse potential fit to the KW potential. They report energy decreases on using a softer wave function of "at least 0.5 °K below energies calculated using" the $u(r)$ of Eq. (3.4) over some unspecified range of densities. Thus we note that although an optimal form for $u(r)$ for the KW potential will be somewhat different than the LJ–WKB form of Eq. (3.4), the change in energies will not be a qualitative effect.

On Fig. 3 we have also shown a curve labeled DEP for H↑. This is the equation of state for the Morse potential fit by DEP to the KW potential (the BBGKY distribution functions have been used). It is clear that the Morse potential yields energies which are much too high because the exponential tail falls off much more rapidly than the exact r^{-6} behavior. The DEP Morse parameters determine an η for H↑ equal to 0.575 which is slightly larger than the 0.55 obtained directly from the KW potential; the difference in energies is much larger than can be accounted for by the difference in eta's.

In MNP it was shown that those LJ systems with $\eta < \eta_{CB} = 0.45$ have a many-body bound state (a liquid); whereas, those with $\eta > \eta_{CB}$ are never bound (a gas). Because of the same low-density behavior in the KW and LJ systems evident from Fig. 3, we can conclude the H↑ ($\eta = 0.55$) will be a zero-temperature gas; whereas, T↑ will be a self-bound liquid. In Table III we list the LJ and KW energies and their kinetic and potential energy

TABLE III. Kinetic, potential, and total energies for the Kolos-Wolniewicz (KW) and Lennard-Jones (LJ) potentials calculated with the BBGKY distribution functions for H↑.

ρ^* (ρr_m^3)	ρ (10^{-3} Å^{-3})	T_{KW} (°K)	V_{KW} (°K)	E_{KW} (°K)	T_{LJ} (°K)	V_{LJ} (°K)	E_{LJ} (°K)
0.01	0.14	0.189	−0.144	0.045	0.200	−0.165	0.035
0.02	0.28	0.393	−0.300	0.094	0.407	−0.333	0.074
0.03	0.42	0.596	−0.450	0.146	0.621	−0.505	0.117
0.04	0.56	0.806	−0.604	0.202	0.843	−0.679	0.164
0.05	0.70	1.022	−0.760	0.262	1.073	−0.856	0.217
0.075	1.06	1.594	−1.161	0.432	1.679	−1.310	0.368
0.10	1.41	2.202	−1.570	0.632	2.330	−1.777	0.553
0.15	2.11	3.538	−2.415	1.12	3.775	−2.744	1.03
0.20	2.82	5.035	−3.280	1.76	5.419	−3.748	1.67
0.25	3.52	6.704	−4.159	2.54	7.262	−4.771	2.49
0.30	4.23	8.556	−5.052	3.50	9.308	−5.798	3.51
0.35	4.93	10.50	−5.853	4.65	11.56	−6.807	4.75
0.40	5.63	12.70	−6.714	5.99	14.04	−7.817	6.22
0.45	6.34	15.03	−7.494	7.54	16.73	−8.802	7.93
0.50	7.04	17.53	−8.228	9.30	19.65	−9.752	9.89

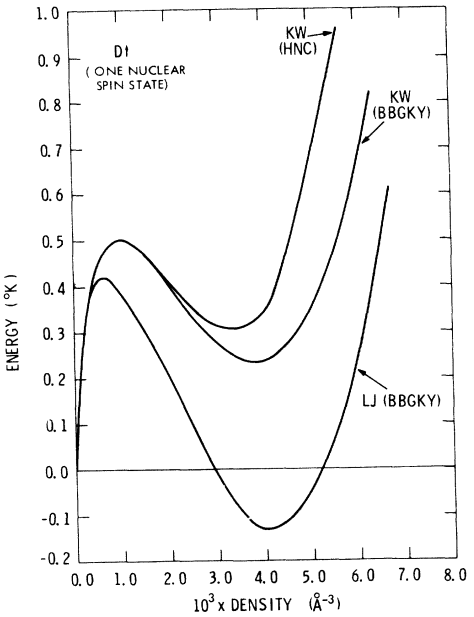

FIG. 4. Energy as a function of density for spin-aligned deuterium with *one* nuclear-spin state. We show calculations for the KW potential with HNC and BBGKY distribution functions and for the LJ potential with the BBGKY distribution function. The KW energies are both in the liquid-gas coexistence region. Note that the energy scale is 0.1 °K; whereas, it is 1.0 °K in Fig. 3.

components for H↑. The dominance of the kinetic energy in this Bose gas is evident.

In Figs. 4 and 5, we display the energies for $D\uparrow_1$ and $D\uparrow_2$, respectively. The most notable feature in both figures is the low-density looping characteristic due to the $\rho^{2/3}$ dependence of the "single-particle" kinetic energy in a Fermi system. We note that the energy scale is a factor of *10* smaller in these figures than in Fig. 3 in order to focus on this interesting "liquid-gas" region. The important difference in these figures is clearly *not* between the HNC and BBGKY results but between the KW and LJ results. The KW equations of state are in the liquid-gas coexistence region as discussed in MNP; whereas, the LJ curves are Fermi liquids. Unfortunately the energies involved are too small to say with certainty whether real $D\uparrow_1$ and $D\uparrow_2$ will be bound or not. There is a possibility that further optimization of the calculation could bring the D↑ energies below zero (similar to the LJ energies) and thus yield a liquid ground state at zero pressure. The effects on the energy of placing all the particles in one spin state can be seen in Table IV. Clearly at each density the energy will be increased by this assignment of spins, however, the effect is very weak except at lowest densities (where the $\rho^{2/3}$ kinetic energy term dominates the energy). It is interesting to note that for $\rho^* \lesssim 0.25$ the ratio of E_1 to E_2 is roughly constant at ~1.8 which is somewhat larger than the ideal gas result of $2^{2/3} \approx 1.6$.

In MNP it was pointed out that at absolute zero fermion systems undergo first order liquid-gas phase transitions when η is viewed as a "conceptual" thermodynamic parameter. Thus, there is a range of η's ($\eta_L \leq \eta \leq \eta_C$) for which the liquid- and gas-phases can coexist. For a system with an η in this range one may go from one phase to the other by changing the pressure. (See, for example Fig. 5 in MNP.) In P-η space, then, η_C is the liquid-gas critical point and η_L is the position of zero-condensation pressure. Clearly, however, since it is the quantum nature which drives this phase transition, by changing the spin distribution one also changes the "position" of the transition. Thus the calculation which was presented in MNP for fermions with two allowed nuclear spin states will have to be redone for fermions with one allowed nuclear spin state. The results of these calculations are shown in Table V. The column of numbers labeled $F2$, refers to the two-spin state parameters calculated in MNP and the column labeled $F1$ is the repeat of the MNP calculation for a single-spin-state system; the equations for this calculation are discussed in the Appendix. On intuitive physical grounds, one might expect

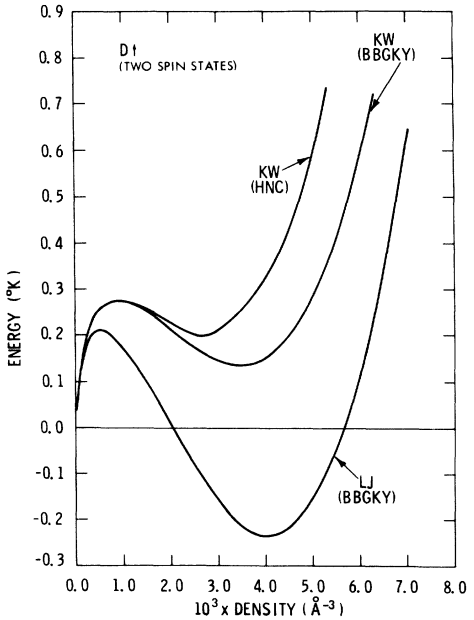

FIG. 5. Energy as a function of density for spin-aligned deuterium with *two* equally populated nuclear-spin states. Results for the KW potential are shown with HNC and BBGKY distribution functions; results for the LJ potential are shown with BBGKY distribution functions. Again the KW energies are both in the liquid-gas coexistence region and the energy scale is 0.1 °K.

TABLE IV. Kinetic, potential, and total energies for D↑ with the Kolos-Wolniewicz potential. Results are shown for deuterium occupying *one* Fermi sea and equally populating *two* Fermi seas. The expectation values were calculated with BBGKY distribution functions.

ρ^* (ρr_m^3)	ρ (10^{-3} Å^{-3})	T_1 (°K)	V_1 (°K)	E_1 (°K)	T_2 (°K)	V_2 (°K)	E_2 (°K)
0.01	0.14	0.305	−0.048	0.256	0.243	−0.096	0.146
0.02	0.28	0.495	−0.132	0.362	0.413	−0.209	0.203
0.03	0.42	0.662	−0.237	0.425	0.573	−0.334	0.238
0.04	0.56	0.821	−0.357	0.464	0.728	−0.468	0.260
0.05	0.70	0.976	−0.489	0.487	0.881	−0.610	0.272
0.075	1.06	1.357	−0.857	0.500	1.261	−0.985	0.276
0.10	1.41	1.741	−1.264	0.477	1.662	−1.402	0.260
0.15	2.11	2.560	−2.171	0.389	2.502	−2.297	0.204
0.20	2.82	3.456	−3.158	0.297	3.415	−3.262	0.152
0.25	3.52	4.440	−4.197	0.243	4.425	−4.292	0.134
0.30	4.23	5.553	−5.304	0.250	5.531	−5.367	0.166
0.35	4.93	6.694	−6.356	0.338	6.680	−6.416	0.264
0.40	5.63	8.069	−7.547	0.522	8.027	−7.581	0.446
0.45	6.34	9.502	−8.683	0.817	9.450	−8.728	0.720
0.50	7.04	11.06	−9.825	1.24	10.98	−9.881	1.10

that

$$\eta_{LF1} < \eta_{LF2}, \tag{3.5a}$$

$$\rho_{LF1} < \rho_{LF2}. \tag{3.5b}$$

The results in Table V confirm (3.5a) but not (3.5b). It turns out that the number of spin states affects not only the Fermi energy, but also the correlations that enter into the calculation of the potential energy and the rest of the kinetic energy. Thus, no simple intuitive picture is available to understand the changes caused by changing the number of allowed nuclear-spin states. This is also true for the thermodynamic parameters at the critical point.

IV. FINITE-TEMPERATURE RESULTS

In this section we shall use the QTCS to make estimates of the critical parameters of D↑$_1$ and D↑$_2$. The estimate of the Bose-Einstein condensation temperature has already been given by SN. To conclude this section we shall discuss the possibility of observing quantum effects on the critical behavior of D↑$_1$ and D↑$_2$.

TABLE V. Critical parameters at zero temperature for Fermi systems with two nuclear-spin states ($F2$) and one nuclear-spin state ($F1$). The results for $F2$ are taken from MNP.

Critical parameter	$F2$	$F1$
η_L	0.290 ± 0.005	0.274
ρ_L^*	0.19 ± 0.02	0.22
η_C	0.33 ± 0.01	0.35
ρ_C^*	0.074 ± 0.004	0.084
P_C^*	0.0013 ± 0.0004	0.0026

In Figs. 6–8 we plot, respectively, as functions of η, the reduced critical temperature T_c^*, the reduced critical pressure P_c^*, and the reduced critical volume V_c^*. The data for ^{3}He, H_2, Ne, and Ar are taken from Refs. 5 and 6. On each figure we also plot η_{CF1} and η_{CF2}. Then we can construct approximate curves for Fermi systems with one allowed nuclear-spin state ($F1$) and two allowed nuclear-spin states ($F2$). The former are shown as dashed lines and the latter as solid lines on Figs. 6–8. The intersection of these curves with

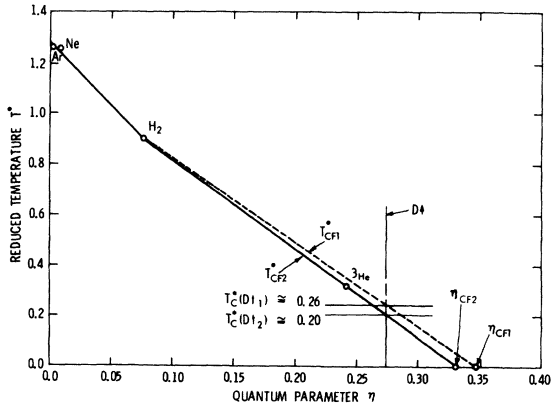

FIG. 6. Reduced critical temperature T_c^* for Fermi systems with one and two nuclear-spin states versus the quantum parameter η. These curves are used to determine T_c^* for D↑$_1$ and D↑$_2$ by graphical construction.

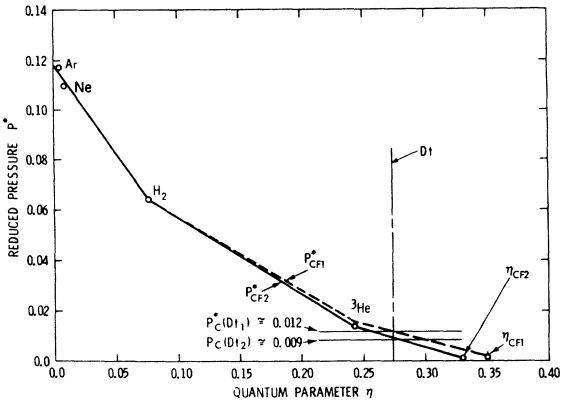

FIG. 7. Reduced critical pressure P_c^* for both Fermi systems versus the quantum parameter η. These curves are used to determine P_c^* for $D\uparrow_1$ and $D\uparrow_2$ by graphical construction.

the line $\eta = 0.274$ (the value for $D\uparrow$) gives the values of these parameters for $D\uparrow_1$ and $D\uparrow_2$. They are summarized in Table VI, where the values for ^{3}He and ^{4}He are also given for comparison. The critical temperatures and pressures for $D\uparrow_1$ and $D\uparrow_2$ are quite a bit lower than those for ^{3}He and ^{4}He as would be expected. However, the critical volumes are much larger. This result is due to the combined effects of the larger η (which increases the quantum mechanical kinetic energy) and the larger value of σ (spin-aligned hydrogen is a much bigger atom than helium).

We shall now turn to discuss the possibility of observing quantum effects on the critical behavior of $D\uparrow_1$ or $D\uparrow_2$. This question has been addressed by Suzuki.[13] He points out that the relevant length

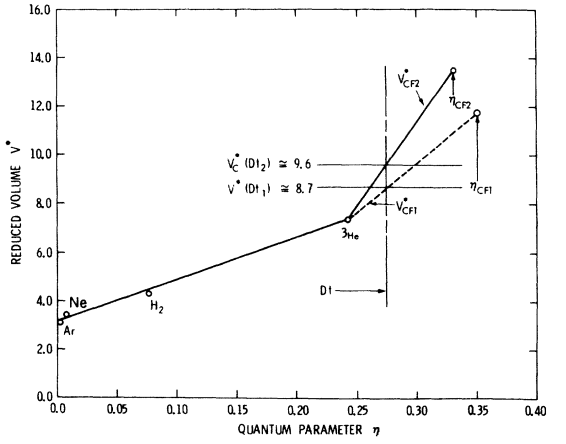

FIG. 8. Reduced critical volume V_c^* for both Fermi systems as a function of the quantum parameter η. These curves are used to determine V_c^* for $D\uparrow_1$ and $D\uparrow_2$ by graphical construction.

TABLE VI. Estimated values of the critical temperature, pressure, and molar volume for $D\uparrow_1$ and $D\uparrow_2$ and the isotopes of He. The values of T_c^*, P_c^*, and V_c^* were obtained by graphical construction as shown on Figs. 6–8.

Property	^{4}He	^{3}He	$D\uparrow_1$	$D\uparrow_2$
T_c^*	0.51	0.33	0.26	0.20
T_c (K)	5.20	3.32	1.68	1.29
P_c^*	0.027	0.014	0.012	0.009
P_c (atm)	2.26	1.15	0.21	0.16
V_c^*	5.89	7.28	8.7	9.6
V_c (cm^3/mole)	59.3	73.23	263.0	290.0

for the critical phenomena is the correlation length ξ; whereas, the relevant length for quantum phenomena is the thermal de Broglie wavelength λ given by

$$\lambda = h/(2\pi m k T)^{1/2} = (2\pi\eta/T^*)^{1/2}\sigma . \qquad (4.1)$$

Thus, on physical grounds one would expect quantum effects to show up when $\lambda \gtrsim \xi$. In order to make this argument quantitative, it would be necessary to construct the proper cross-over scaling function and this has not yet been done. Nevertheless, the essence of the physics has been given by Suzuki and it is worthwhile to look at the relevant numbers. Values for λ for various substances at T_c^* are shown on Table VII. Even though the values of λ_c for $D\uparrow_1$ and $D\uparrow_2$ are both about 10 Å, it seems unlikely that this is large enough to affect the critical behavior. After all experiments routinely get to within 10^{-3} °K of the critical point where it is expected that $\xi \sim 10^2$ Å, so that $\xi \gg \lambda$ in each case. Of course, there exist corrections to the leading singular term and these might be influenced by quantum effects. Nevertheless, it is our opinion that it is unlikely that quantum effects or critical behavior can be observed, at least in the most singular term in the thermodynamic quantity under observation.

TABLE VII. Thermal de Broglie wavelength at the critical point λ_c for various substances. The data for T_c^* are taken from Refs. 5 and 6.

Substance	T_c^*	λ_c (Å)
^{3}He	0.33	5.47
^{4}He	0.51	3.82
H_2	0.90	2.13
Ne	1.25	0.57
Ar	1.26	0.23
$D\uparrow_1$	0.26	9.5
$D\uparrow_2$	0.20	10.8

ACKNOWLEDGMENTS

The authors wish to acknowledge several illuminating conversations with Professor William C. Stwalley in the early stages of this work. They also wish to thank Brookhaven National Laboratory for its hospitality during part of this work. Finally, they wish to thank the University Computer Center of the University of Massachusetts for computing support.

APPENDIX

In this section we shall write down those equations needed to evaluate the ground-state energies for the D↑ systems. We first write the energy per particle in terms of the kinetic and potential energies

$$E(\rho,\eta,\delta)=\eta\,\langle t/N\rangle+\langle v/N\rangle\,, \tag{A1}$$

where ρ is the density, η is the quantum parameter, and δ is the parameter which measures the spin distribution. The brackets represent averages defined by

$$\langle v/N\rangle=\tfrac{1}{2}\rho\int g_F(r)\,v(r)\,d\vec{\mathbf{r}}\,, \tag{A2}$$

$$\langle t/N\rangle=-\frac{1}{2N}\sum_{i=1}^{N}\frac{\int\psi^*\nabla_i^2\psi\,d\vec{\mathbf{r}}^N}{\int|\psi|^2\,d\vec{\mathbf{r}}^N}\,. \tag{A3}$$

In order to calculate the average potential energy, Eq. (A2), one needs to know the fermion radial distribution function $g_F(r)$ which is defined by

$$g_F(r_{12})=\frac{N(N-1)}{\rho^2}\frac{\int|\psi|^2 d\vec{\mathbf{r}}_3\cdots d\vec{\mathbf{r}}_N}{\int|\psi|^2 d\vec{\mathbf{r}}^N}\,. \tag{A4}$$

The presence of the Slater determinant in the wave function makes the calculation of $g_F(r)$ quite difficult. Thus, Wu and Feenberg[12] introduced a cluster-expansion procedure in order to account for the statistical effects in the Slater determinant. The cluster expansion necessarily depends on the distribution of spins and thus on δ. The parameter δ counts the number of *equally* populated Fermi seas; thus, $\delta=1,2$ for $D\uparrow_1$ and $D\uparrow_2$, respectively. The kinetic energy, Eq. (A3), can also be developed in a "statistical" cluster expansion. Due to the Laplacian operator, however, the expansion is somewhat more complicated than for the potential energy.

Thus writing down the required cluster expansion yields

$$g_F(r_{12})=g_B(r_{12})\,[1+F^{(2)}(r_{12})+F^{(3)}(r_{12})+\cdots]\,, \tag{A5}$$

$$\langle t/N\rangle=\tfrac{1}{4}\langle\nabla^2 u(r)\rangle+E_{1F}+E_{2F}+E_{3F}+\cdots\,, \tag{A6}$$

where the nth terms in Eqs. (A5) and (A6) represent the contribution from n-particle exchange in the Slater determinant. The first term in Eq. (A6), the correlational kinetic energy, is in the same form as the potential energy, Eq. (A2), and so it requires $g_F(r)$ in order to be determined. In Eq. (A5) the function $g_B(r)$ is the "boson" distribution function calculated with the F part of ψ only, see Eq. (3.1). The remaining terms in Eq. (A5) are defined by

$$F^{(2)}(r_{12})=-l^2(y_{12})/\delta \tag{A7}$$

$$F^{(3)}(r_{12})=-\frac{2\rho}{\delta}\int g_B(r_{23})h(r_{13})\,l^2(y_{23})\,d\vec{\mathbf{r}}_3+\frac{2\rho}{\delta^2}l(y_{12})\int g_B(r_{23})h(r_{13})\times l(y_{13})\,l(y_{23})\,d\vec{\mathbf{r}}_3 \tag{A8}$$

and we have used

$$h(r)=g_B(r)-1, \tag{A9}$$

$$l(y)=3[\sin(y)-y\cos(y)]/y^3\,, \tag{A10}$$

$$y=k_F r=(6\pi^2\rho/\delta)^{1/3}r\,. \tag{A11}$$

The series is truncated after the $n=3$ term, $F^{(3)}$, which used the Kirkwood superposition approximation[12] for the three-particle distribution functions.

The terms in the kinetic energy series, Eq. (A6), are given by

$$E_{1F}=\tfrac{3}{10}k_F^2\,, \tag{A12}$$

$$E_{2F}=(40E_{1F}/\delta)\int_0^1 u(2k_F s)(1-\tfrac{3}{2}x+\tfrac{1}{2}x^3)\,x^4\,dx\,, \tag{A13}$$

$$E_{3F}=-\left(\frac{10E_{1F}}{3\delta^2}\right)\left(\frac{3}{8\pi}\right)^3\int x_{12}^2 S(x_{12}k_F)\,u(x_{13}k_F)\times u(x_{23}k_F)\,d\vec{\mathbf{x}}_1 d\vec{\mathbf{x}}_2 d\vec{\mathbf{x}}_3\,, \tag{A14}$$

and

$$u(k)=S(k)-1=\rho\int e^{i\vec{\mathbf{k}}\cdot\vec{\mathbf{r}}}h(r)\,d\vec{\mathbf{r}}\,. \tag{A15}$$

The kinetic energy series was truncated after the $n=3$ term, E_{3F}, which was evaluated by using the convolution approximation for the three-particle distribution function and a quadratic approximation for $S(k)$.[12]

*This research was supported, in part, by the NSF under Grant Nos. DMR76-14447 and DMR73-02609.
†This research was performed as part of the NSF Independent Research Program. However, any of the opinions expressed herein are those of the author and do not necessarily reflect the views of the NSF.

[1]J. V. Dugan and R. D. Etters, J. Chem. Phys. 59, 6171 (1973); R. D. Etters, J. V. Dugan, and R. W Palmer, *ibid.* 62, 313 (1975); R. D. Etters, Phys. Lett. 42A, 439 (1973); R. L. Danilowicz, J. V. Dugan, and R. D. Etters, J. Chem. Phys. 65, 498 (1976); we shall refer to these references collectively as DEP.
[2]W. C. Stwalley and L. H. Nosanow, Phys. Rev. Lett. 36, 910 (1976); we shall refer to this reference as SN.
[3]L. H. Nosanow, L. J. Parish, and F. J. Pinski, Phys. Rev. B 11, 191 (1975).
[4]M. D. Miller, L. H. Nosanow, and L. J. Parish, Phys. Rev. Lett. 35, 581 (1975); M. D. Miller, L. H. Nosanow, and L. J. Parish, Phys. Rev. B 15, 214 (1976); we shall refer to this work as MNP.
[5]L. H. Nosanow, J. Low Temp. Phys. 23, 605 (1976).
[6]L. H. Nosanow, J. Low Temp. Phys. 26, 613 (1977).
[7]J. de Boer, Physica 14, 139 (1948).
[8]J. de Boer and B. S. Blaisse, Physica 14, 149 (1948); J. de Boer and R. J. Lunbeck, *ibid.* 14, 520 (1948).
[9]W. Kolos and L. Wolniewicz, J. Chem. Phys. 43, 2429 (1965); Chem. Phys. Lett. 24, 457 (1974).
[10]R. J. Bell, Proc. Phys. Soc. Lond. 87, 594 (1966).
[11]For a discussion of the BBGKY-KSA and HNC integral equation and their numerical solution see, e.g., M. D. Miller, Phys. Rev. B 14, 3937 (1976).
[12]F. Y. Wu and E. Feenberg, Phys. Rev. 128, 943 (1962).
[13]M. Suzuki, Prog. Theor. Phys. 56, 77 (1976).